Inorg. Chem. **2007**, *46*, 3450–3458

Two- and Three-Dimensional Lanthanide Complexes: Synthesis, Crystal Structures, and Properties

Jun Xia, Bin Zhao, Hong-Sheng Wang, Wei Shi, Yue Ma, Hai-Bin Song, Peng Cheng,* Dai-Zheng Liao, and Shi-Ping Yan

Department of Chemistry, Nankai University, Tianjin 300071, People's Republic of China

Received August 28, 2006

3,5-Pyrazoledicarboxylic acid (H_3L) reacts with nitrate salts of lanthanide(III) (Ln = Pr, Nd, Sm, Eu, Gd, Tb, Dy, Ho, and Er) under hydrothermal conditions to form a series of lanthanide polymers **1**–**9**. These nine polymers have the same crystal system of monoclinic, but they exhibit three different kinds of metal–organic framework structures. The complexes $\{[Ln_2(HL)_3(H_2O)_4]\cdot 2H_2O\}_n$ (Ln = Pr (**1**), Nd (**2**), and Sm (**3**)) were isostructural and exhibited porous 3D frameworks with a *Cc* space group. The complexes $\{[Ln_2(HL)_3(H_2O)_3]\cdot 3H_2O\}_n$ (Ln = Eu (**4**), Gd (**5**), and Tb (**6**)) were isostructural and built 2D double-decker (2DD) frameworks with a $P2_1/c$ space group. The complexes $\{[Ln(HL)(H_2L)(H_2O)_2]\}_n$ ((Ln = Dy (**7**), Ho (**8**), and Er (**9**)) were also isostructural and formed 2D monolayer (2DM) frameworks with a $P2_1/n$ space group. The structure variation from the 3D porous framework to the 2D double-decker to the 2D monolayer is attributed to the lanthanide contraction effect. Notably, six new coordination modes of 3,5-pyrazoledicarboxylic acid were observed, which proved that 3,5-pyrazoledicarboxylic acid may be used as an effective bridging ligand to assemble lanthanide-based coordination polymers. The photophysical and magnetic properties have also been investigated.

Introduction

In recent years, increasing attention has been paid to the design and synthesis of lanthanide-based metal−organic frameworks (MOFs) due to their unusual coordination characteristics and exceptional optical and magnetic properties.[1−6] Compared to transition metals, lanthanides have much higher coordination numbers and more flexible coordination geometry, which make it difficult to control the preparation of lanthanide complexes but are helpful in the formation of unusual MOF architectures.[7−9] The reported MOFs based on lanthanides possess beautiful and interesting topological structures, such as 1D chains,[10] 2D grids,[11] 3D porous structures, and interpenetrating networks.[12] On the other hand, for lanthanide compounds, it is well-known that they exhibit excellent photophysical properties, which can contribute to *f*−*f* transitions with an extremely narrow bandwidth.[13] Combining the above two points, the MOFs based on lanthanides have great potential applications, such as catalysis, adsorption, magnetic materials, separation sensors, luminescent sensors, and so on.[14−17] Therefore, design and

* To whom correspondence should be addressed. Fax: +86-2223502458. E-mail: pcheng@nankai.edu.cn.

(1) Kido, J.; Okamoto, Y. *Chem. Rev.* **2002**, *102*, 2357.
(2) Marques, N.; Sella, A.; Takats, J. *Chem. Rev.* **2002**, *102*, 2137.
(3) Bochkarev, M. N. *Chem. Rev.* **2002**, *102*, 2089.
(4) (a) Petoud, S.; Cohen, S. M.; Bunzli, J.-C. G.; Raymond, K. N. *J. Am. Chem. Soc.* **2003**, *125*, 13324. (b) Ishikawa, N.; Sugita, M.; Ishikawa, T.; Koshihara, S.-Y.; Kaizu, Y. *J. Am. Chem. Soc.* **2003**, *125*, 8694.
(5) Zaleski, C. M.; Depperman, E. C.; Kampf, J. W.; Kirk, M. L.; Pecoraro, V. L. *Angew. Chem., Int. Ed.* **2004**, *43*, 3912.
(6) Hamada, T.; Manabe, K.; Ishikawa, S.; Nagayama, S.; Shiro, M.; Kobayashi, S. *J. Am. Chem. Soc.* **2003**, *125*, 2989.
(7) Devic, T.; Serre, C.; Audebrand, N.; Marrot, J.; Ferey, G. *J. Am. Chem. Soc.* **2005**, *127*, 12788.
(8) Ghosh, S. K.; Bharadwaj, P. K. *Inorg. Chem.* **2004**, *43*, 2293.
(9) Lill, D. T.; Gunning, N. S.; Cahill, C. L. *Inorg. Chem.* **2005**, *44*, 258.
(10) (a) Shin, D. M.; Lee, I. S.; Lee, Y. A.; Chung, Y. K. *Inorg. Chem.* **2003**, *42*, 2977. (b) Withersby, M. A.; Blake, A. J.; Champness, N. R.; Hubberstey, P.; Li, W. S.; Schröder, M. *Angew. Chem., Int. Ed. Engl.* **1997**, *39*, 2327. (c) Batsanov, A. S.; Begley, M. J.; Hubberstey, P.; Stroud, J. *J. Chem. Soc., Dalton Trans.* **1996**, 1947.
(11) (a) Withersby, M. A.; Blake, A. J.; Champness, N. R.; Cooke, P. A.; Hubberstey, P.; Li, W. S.; Schröder, M. *Inorg. Chem.* **1999**, *38*, 2259. (b) Nomiya, K.; Yokoyama, H. *J. Chem. Soc., Dalton Trans.* **2002**, 2483.
(12) (a) Shin, D. M.; Lee, I. S.; Chung, Y. K.; Lah, M. S. *Inorg. Chem.* **2003**, *42*, 5459. (b) Mitsurs, K.; Shimamura, M.; Noro, S. I.; Minakoshi, S.; Asami, A.; Seki, K.; Kitagawa, S. *Chem. Mater.* **2000**, *12*, 1288. (c) Carlucci, L.; Ciani, G.; Proserpio, D. M. *J. Chem. Soc., Dalton Trans.* **1999**, 1799. (d) He, C.; Zhang, B. G.; Duan, C. Y.; Li, J. H.; Meng, Q. J. *Eur. J. Inorg. Chem.* **2000**, 2549.
(13) (a) Sabbatini, N.; Guardigi, M.; Bolletta, F.; Manet, I.; Ziessel, R. *Angew. Chem., Int. Ed. Engl.* **1994**, *33*, 1501. (b) Yang, X.-P.; Jones, R. A. *J. Am. Chem. Soc.* **2005**, *127*, 7686.

10.1021/ic061620p CCC: $37.00
Published on Web 01/23/2007

synthesis of lanthanide-based coordination polymers which have novel topological structures and unique magnetic or luminescent properties is a promising work and attracts more and more attention.

However, in the synthesis of lanthanide-based MOFs, the judicious choice of the organic linker plays a key role in the structural assembly. Many chemists synthesize these MOFs with a lot of different carboxylic acids, such as aromatic acids,[18a] aliphatic acids,[18b] and heterocyclic acids.[18c] Among those acids, the pyridinecarboxylic acids, such as pyridine-2,6-dicarboxylic acid, pyridine-2,5-dicarboxylic acid, and so on, have been investigated widely,[19] and our team has also focused on this topic for a long time and made some progress.[20] On the basis of the above achievements, we just paid attention to the pentaheterocyclic acid, 3,5-pyrazoledicarboxylic acid (H_3L), as the multifunctional ligand. The selection of ligand was based on the following considerations: (i) the flexible and multifunctional coordination sites may generate multidimensional structures; (ii) it can be deprotonated to H_2L^- and HL^{2-}, which provide more coordination modes; and (iii) the lanthanide complexes of 3,5-pyrazoledicarboxylic acid have not been reported before, to the best of our knowledge.

By reacting H_3L with the corresponding lanthanide(III) nitrates under hydrothermal conditions, we obtained a series of coordination polymers, **1**−**9**. Among the nine polymers, complexes **1**−**3** are isostructural with *Cc* space group, and isostructural complexes **4**−**6** and **7**−**9** belong to the $P2_1/c$ and $P2_1/n$ space groups, respectively. An interesting phenomenon was observed; the structures of the nine polymers varied regularly with increasing atomic number of lanthanide. The complexes **1**−**3** displayed porous 3D frameworks; the complexes **4**−**6** showed 2D double-decker structures (2DD); and the complexes **7**−**9** formed 2D monolayer frameworks (2DM). With the atomic numbers increasing, the structure of nine complexes changed in the order of 3D → 2DD → 2DM, and the coordination number of lanthanide decreased, which can be attributed to the lanthanide contract effect. Complexes **3**, **4**, **6**, and **7** showed the characteristic emissions for Sm^{3+}, Eu^{3+}, Tb^{3+}, and Dy^{3+}, respectively, and complex **5** exhibited a weak antiferromagnetic interaction between Gd^{3+} ions.

Experimental Section

Materials and Physical Techniques. All reagents and solvents employed were commercially available and used as received without further purification. H_3L was synthesized according to the literature method.[21] The purity was determined by elemental analysis, ^1H NMR, and IR. The lanthanide(III) nitrates were prepared by dissolving corresponding lanthanide oxides (General Research Institute for Nonferrous Metals, 99.99%) in nitric acid followed by recrystallization and drying. The syntheses of **1**−**9** were carried out in 20 mL Teflon-lined autoclaves under autogenous pressure. Elemental analysis for C, H, and N was obtained at the Institute of Elemental Organic Chemistry, Nankai University. The FT−IR spectra were measured with a Bruker Tensor 27 spectrometer on KBr disks. The fluorescent spectra were measured on a Varian Cary Eclipse Fluorescence spectrophotometer. The variable-temperature magnetic susceptibilities in the temperature range of 5−300 K were measured on a Quantum Design MPMS-7 SQUID magnetometer in a field of 1 T. Diamagnetic corrections were made with Pascal's constants for all of the constituent atoms.

Synthesis of $\{[Ln_2(HL)_3(H_2O)_4]\cdot 2H_2O\}_n$ (Ln = Pr (1), Nb (2), and Sm (3)). A mixture of H_3L (0.078 g, 0.50 mmol), 0.30 mmol of $Ln(NO_3)_3\cdot 6H_2O$ (0.130 g (**1**), 0.131 g (**2**), 0.133 g (**3**)), 0.1 mL of HCl (3 M), and H_2O (10 mL) was placed in a 20 mL acid digestion bomb, and the pH value was 2. It was heated at 180 °C for 3 days; the suitable crystals of **1**−**3** were obtained when cooling to room temperature. For **1**, yield: 0.040 g, 31% based on Pr. Anal. Calcd (%) for $C_{15}H_{18}N_6Pr_2O_{18}$: C, 21.12; H, 2.11; N, 9.86. Found: C, 21.13; H, 2.07; N, 10.13. For **2**, yield: 0.045 g, 35% based on Nd. Anal. Calcd (%) for $C_{15}H_{18}N_6Nb_2O_{18}$: C, 20.96; H, 2.10; N, 9.78. Found: C, 20.80; H, 2.17; N, 10.05. For **3**, yield: 0.039 g, 30% based on Sm. Anal. Calcd (%) for $C_{15}H_{18}N_6Sm_2O_{18}$: C, 20.66; H, 2.07; N, 9.64. Found: C, 20.51; H, 2.07; N, 9.77.

Synthesis of $\{[Ln_2(HL)_3(H_2O)_3]\cdot 3H_2O\}_n$ (Ln = Eu (4), Gd (5), and Tb (6)). An identical procedure as that for **1**−**3** was followed to prepare **4** and **5**, except that lanthanide(III) nitrates were replaced by $Ln(NO_3)_3\cdot 6H_2O$ [Ln = Eu (**4**), Gd (**5**), and Tb (**6**)]. For **4**, yield: 0.026 g, 20% based on Eu. Anal. Calcd (%) for $C_{15}H_{18}N_6Eu_2O_{18}$: C, 20.59; H, 2.06; N, 9.61. Found: C, 20.53; H, 2.06; N, 9.88. For **5**, yield: 0.026 g, 20% based on Gd. Anal. Calcd (%) for $C_{15}H_{18}N_6Gd_2O_{18}$: C, 20.34; H, 2.03; N, 9.49. Found: C, 19.92; H, 2.52; N, 9.47. For **6**, yield: 0.031 g, 23% based on Tb. Anal. Calcd (%) for $C_{15}H_{18}N_6Tb_2O_{18}$: C, 20.27; H, 2.03; N, 9.46. Found: C, 19.84; H, 2.33; N, 9.87.

Synthesis of $\{[Ln(HL)(H_2L)(H_2O)_2]\}_n$ (Ln = Dy (7), Ho (8), and Er (9)). An identical procedure to that of **1**−**3** was followed to prepare **7**−**9**, except that lanthanide(III) nitrates were replaced by $Ln(NO_3)_3\cdot 6H_2O$ [Ln = Dy (**7**), Ho (**8**), and Er (**9**)]. For **7**, yield: 0.044 g, 29% based on Dy. Anal. Calcd (%) for $C_{10}H_9N_4$-

(14) (a) Harrison, B. S.; Foley, T. J.; Knefely, A. S.; Mwaura, J. K.; Cunningham, G. B.; Kang, T. S.; Bouguettaya, M.; Boncella, J. M.; Reynolds, J. R.; Schanze, K. S. *Chem. Mater.* **2004**, *16*, 2938. (b) He, H. S.; Guo, J. P.; Zhao, Z. X.; Wong, W. K.; Wong, W. Y.; Lo, W. K.; Li, K. F.; Luo, L.; Cheah, K. W. *Eur. J. Inorg. Chem.* **2004**, 837. (c) Parkar, D. *Coord. Chem. Rev.* **2000**, *205*, 109. (d) Morrish, A. H. *The Physical Principles of Magnetism*; Wiley: New York, 1965.

(15) (a) Dickins, R. S.; Gaillard, S.; Hughes, S. P.; Badari, A. *Chirality* **2005**, *17*, 357. (b) Yao, Y. M.; Zhang, Z. Q.; Peng, H. M.; Zhang, Y.; Shen, Q.; Lin, J. *Inorg. Chem.* **2006**, *45*, 2175. (c) Wang, S. W.; Zhou, S. L.; Sheng, E. H.; Xie, M. H.; Zhang, K. H.; Cheng, L.; Feng, Y.; Mao, L. L.; Huang, Z. X. *Organometallics* **2003**, *22*, 3546. (d) Tobisch, S. *J. Am. Chem. Soc.* **2005**, *127*, 11979.

(16) (a) Pan, L.; Adams, K. M.; Hernandez, H. E.; Wang, X.; Zheng, C.; Hattori, Y.; Kaneko, K. *J. Am. Chem. Soc.* **2003**, *125*, 3062. (b) Gunnlaugsson, T.; Leonard, J. P.; Senechal, K.; Harte, A. J. *J. Am. Chem. Soc.* **2003**, *125*, 12062.

(17) (a) Kuriki, K.; Koike, Y.; Okamoto, Y. *Chem. Rev.* **2002**, *102*, 2347. (b) Tsukube, H.; Shinoda, S. *Chem. Rev.* **2002**, *102*, 2389.

(18) (a) Chen, X. Y.; Zhao, B.; Shi, W.; Xia, J.; Cheng, P.; Shi, W.; Liao, D. Z.; Yan, S. P.; Jiang, Z. H. *Chem. Mater.* **2005**, *17*, 2866. (b) Daniel, T. L.; Noel, S. G.; Christopher, L. C. *Inorg. Chem.* **2005**, *44*, 258. (c) Pavel, V.; Peter, C.; Jan, K.; Jakub, R.; Peter, H.; Ivan, L. *Inorg. Chem.* **2005**, *44*, 5591.

(19) (a) Sujit, K. G.; Parimal, K. B. *Inorg. Chem.* **2003**, *42*, 8250. (b) Qin, C.; Wang, X. L.; Wang, E. B.; Su, Z. M. *Inorg. Chem.* **2005**, *44*, 7122.

(20) (a) Zhao, B.; Gao, H. L.; Chen, X. Y.; Cheng, P.; Shi, W.; Liao, D. Z.; Yan, S. P.; Jiang, Z. H. *Chem.—Eur. J.* **2006**, *12*, 149. (b) Zhao, B.; Yi, L.; Dai, Y.; Chen, X. Y.; Cheng, P.; Shi, W.; Liao, D. Z.; Yan, S. P.; Jiang, Z. H. *Inorg. Chem.* **2005**, *44*, 911. (c) Zhao, B.; Cheng, P.; Chen, X. Y.; Cheng, C.; Shi, W.; Liao, D. Z.; Yan, S. P.; Jiang, Z. H. *J. Am. Chem. Soc.* **2004**, *126*, 3012. (d) Zhao, B.; Chen, X. Y.; Cheng, P.; Liao, D. Z.; Yan, S. P.; Jiang, Z. H. *J. Am. Chem. Soc.* **2004**, *126*, 15394. (e) Gao, H. L.; Yi, L.; Zhao, B.; Zhao, X. Q.; Cheng, P.; Liao, D. Z.; Yan, S. P. *Inorg. Chem.* **2006**, *45*, 5980.

(21) Ho, H. L.; Bruce, F. C.; William, A. D. *J. Org. Chem.* **1989**, *54*, 428.

DyO_{10}: C, 23.64; H, 1.77; N, 11.03. Found: C, 23.57; H, 1.84; N, 11.23. For **8**, yield: 0.040 g, 26% based on Ho. Anal. Calcd (%) for $C_{10}H_9N_4HoO_{10}$: C, 23.52; H, 1.76; N, 10.98. Found: C, 23.12; H, 2.11; N, 11.02. For **9**, yield: 0.042 g, 27% based on Er. Anal. Calcd (%) for $C_{10}H_9N_4ErO_{10}$: C, 23.51; H, 1.76; N, 10.97. Found: C, 23.10; H, 2.00; N, 11.27.

Crystallographic Analyses. Crystallographic data of **1**−**9** were collected at 293 K on a Bruker SMART 1000 CCD diffractometer with Mo Kα monochromated radiation ($\lambda = 0.71073$ Å) using the $\omega-\varphi$ scan technique. An empirical absorption correction was applied. The structures were solved by direct methods and refined by full-matrix least squares against F^2 using the SHELXS-97 and SHELXL-97 programs.[22,23] Anisotropic thermal parameters were assigned to all non-hydrogen atoms. The hydrogen atoms were set in calculated positions and refined as riding atoms with a common fixed isotropic thermal parameter. Analytical expressions of neutral atom scattering factors were employed, and anomalous dispersion corrections were incorporated. The crystallographic data and selected bond lengths for **1**−**9** are listed in Table 1. CCDC 614525 (**1**), 614526 (**2**), 614527 (**3**), 614528 (**4**), 614529 (**5**), 614530 (**6**), 614531 (**7**), 614532 (**8**), and 614533 (**9**) contain the supplementary crystallographic data. These data can be obtained free of charge via www.ccdc.cam.ac.uk/conts/retrieving.html (or from the Cambridge Crystallographic Data Center, 12 Union Road, Cambridge CB2 1EZ, UK; fax: (+44) 1223−336-033. E-mail: deposit@ccdc.cam.ac.uk).

Results and Discussion

Synthesis. The crystals of **1**−**9** were successfully synthesized by reacting H_3L with the corresponding lanthanide nitrates at 180 °C for 3 days under hydrothermal conditions. The suitable crystals were not obtained when we tried to synthesize the complexes by traditional methods such as slow evaporating and diffusing at room temperature. This may be ascribed to the features of hydrothermal synthesis, a special environment with high temperature and pressure, which encouraged the generation of large crystals. On the other hand, we found the pH value was very important to form suitable crystals. If the pH value was 4, the crystals were small with some powder production. When the pH value was adjusted to 2 via the addition of hydrochloric acid (3 M), the crystals were larger for crystallographic analyses, and the powder disappeared.

The IR spectra of complexes **1**−**9** have been measured. The IR spectra of **1**−**3** are fully identical. This indicates that the three complexes may be isostructural, which was further confirmed by the X-ray diffraction analysis. As expected, it is the same with **4**−**6** and **7**−**9**. For example, the characteristic bands of the carboxylate groups in **1**−**3** are all at ca. 1592 cm^{-1} for asymmetric stretching and 1491 and 1465 cm^{-1} for symmetric stretching. The asymmetric stretching vibrations of the carboxylate groups in **4**−**6** were observed at 1585 cm^{-1} as a broad band, and the band of symmetric stretching vibrations was observed at 1442 cm^{-1}. The signals in **7**−**9** at 1593 and 1496 cm^{-1} correspond to the asymmetric and symmetric stretching vibrations of carboxylate groups,

Table 1. Crystal Data and Structure Refinement for **1**−**9**

	1	**2**	**3**	**4**	**5**	**6**	**7**	**8**	**9**
empirical formula	$C_{15}H_{18}N_6O_{18}Pr_2$	$C_{15}H_{18}N_6O_{18}Nb_2$	$C_{15}H_{18}N_6O_{18}Sm_2$	$C_{15}H_{18}N_6O_{18}Eu_2$	$C_{15}H_{18}N_6O_{18}Gd_2$	$C_{15}H_{18}N_6O_{18}Tb_2$	$C_{10}H_9N_4O_{10}Dy$	$C_{10}H_9N_4O_{10}Ho$	$C_{10}H_9N_4O_{10}Er$
M	852.17	858.83	871.05	874.28	884.85	888.20	507.71	510.14	510.46
T/K	293(2)	293(2)	293(2)	294(2)	294(2)	294(2)	293(2)	293(2)	294(2)
λ/Å	0.71073	0.71073	0.71073	0.71073	0.71073	0.71073	0.71073	0.71073	0.71073
cryst syst	monoclinic	monoclinic	monoclinic	monoclinic	monoclinic	monoclinic	monoclinic	monoclinic	monoclinic
space group	*Cc*	*Cc*	*Cc*	$P2_1/c$	$P2_1/c$	$P2_1/c$	$P2_1/n$	$P2_1/n$	$P2_1/n$
a/Å	15.6873(13)	15.648(2)	15.543(3)	10.941(3)	10.9880(18)	10.9584(12)	10.862(3)	10.861(6)	10.8421(3)
b/Å	8.8288(7)	8.8089(13)	8.7650(15)	10.169(2)	10.2056(17)	10.1701(11)	9.282(3)	9.295(5)	9.2566(11)
c/Å	18.3278(15)	18.303(3)	18.219(3)	10.546(3)	10.5712(17)	10.5284(12)	14.230(4)	14.259(7)	14.2362(17)
α/°	90	90	90	90	90	90	90	90	90
β/°	98.4240(10)	98.421(2)	98.372(2)	100.130	100.224(2)	100.2360(10)	104.968(4)	104.901(7)	104.872(2)
γ/°	90	90	90	90	90	90	90	90	90
V/Å^3	2511.0(4)	2495.7(6)	2455.7(7)	1155.0(5)	1166.6(3)	1154.7(2)	1386.1(7)	1391.0(12)	1380.9(3)
Z	4	4	4	2	2	2	4	4	4
μ/mm^{-1}	3.932	4.213	4.835	5.487	5.741	6.181	5.461	4.280	6.148
R1 [$I > 2\sigma(I)$]	0.0174	0.0160	0.0149	0.0230	0.0201	0.0188	0.0251	0.0162	0.0273
wR2	0.0405	0.0356	0.0318	0.0547	0.0481	0.0448	0.0610	0.0366	0.0714

(22) Sheldrick, G. M. *SHELXS 97, Program for the Solution of Crystal Structures*; University of Göttingen: Germany, 1997.
(23) Sheldrick, G. M. *SHELXL 97, Program for the Refinement of Crystal Structures*; University of Göttingen: Germany, 1997.

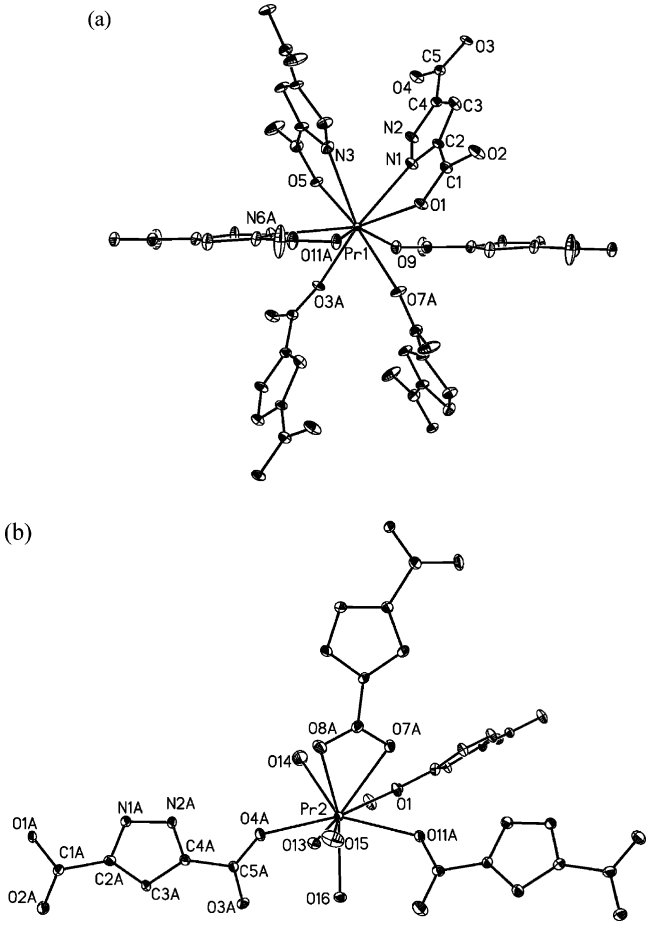

Figure 1. The coordination environments of Pr1 (a) and Pr2 (b) in **1**. Hydrogen atoms have been omitted for clarity.

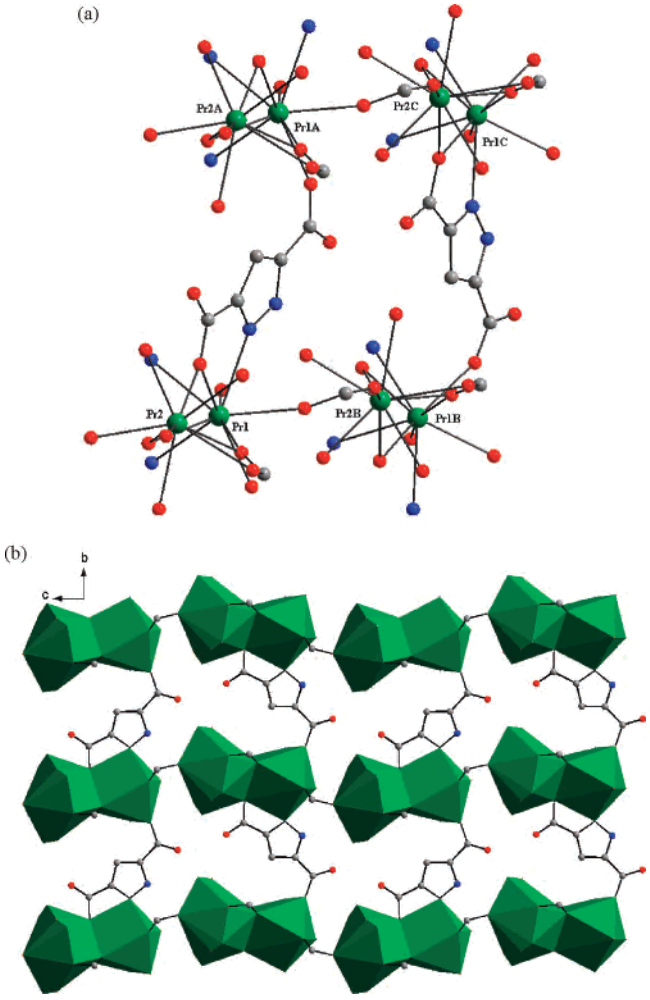

Figure 2. (a) The Pr_8 unit in complex **1**. (b) 2D grid motif in the *bc* plane. Pr, green; O, red; N, blue; C, gray.

respectively. Interestingly, in **7**−**9**, a sharp peak can be observed at 1706 cm^{-1}, which can be assigned to the free carboxylate groups. The result of crystallographic analyses also shows that carboxylate groups of H_3L ligands do not coordinate completely.

Crystal Structures of 1−3. The X-ray structure analyses reveal that **1**−**3** are isomorphic; here, complex **1** is taken as an example to depict the three-dimensional structure in detail. Two crystallographically independent Pr atoms (Pr1 and Pr2) in **1** are observed (Figure 1). Pr1 is coordinated with three nitrogen atoms and six oxygen atoms from six HL anions which have two different coordination modes. Three HL anions coordinate to Pr1 with both nitrogen and oxygen atoms at the same time; the others only coordinate to Pr1 with oxygen atoms. Among the ligands, three crystallographically independent HL anions are observed. The dihedral angles between adjacent pyrazole rings are 61.8, 119.6, and 57.8°. Pr2 is coordinated with nine oxygen atoms; five oxygen atoms are from four HL anions, and the others are from water molecules. Among the four HL anions, one anion chelates to Pr2 with two oxygen atoms at the same time, and the others coordinate to Pr2 with one oxygen atom. Thus, both Pr atoms are nine coordinated with the coordination geometry of a distorted tricapped trigonal. Furthermore, Pr1 and Pr2 are linked together to form a binuclear unit by three μ_2-O bridges which are from HL anions. The distance between two Pr atoms is 4.021(1) Å, which is similar to that of the reported Pr complex,[24] and four units are bridged via HL^{2-} and $\mu_{1,3}$-O bridges to form a unique octanuclear homometallic Pr_8 cluster in the *bc* plane (Figure 2a). In the Pr_8 cluster, Pr1C and Pr1B (Pr1A and Pr1) are linked by an HL anion, while Pr1A and Pr2C (Pr1 and Pr2B) are linked by a $\mu_{1,3}$-O bridge. The eight Pr atoms form two identical parallelograms. Pr1, Pr1A, Pr2, and Pr2A atoms are coplanar strictly and form one parallelogram: Pr1−Pr1A (Pr2−Pr2A), 8.829(1) Å; Pr1−Pr2 (Pr1A−Pr2A), 4.021(1) Å; Pr2−Pr1−Pr1A (Pr1A−Pr2A−Pr2), 95.18°; Pr1−Pr1A−Pr2A (Pr2A−Pr2−Pr1), 84.82°. The other four Pr atoms (Pr1B, Pr1C, Pr2B, and Pr2C) form another parallelogram. The dihedral angle between two parallelograms is 9.1°. Most interestingly, viewed in the *bc* plane, the Pr_8 cluster as a building block is further assembled into a wonderful 2D grid (Figure 2b). Along the *a* axis, two adjacent Pr_8 clusters are linked together with double HL anion bridges; therefore, the 2D grid is further assembled into a spectacular 3D framework (Figure 3).

Because the H_3L has two nitrogen atoms and four oxygen atoms which can be coordinated with metal centers, the coordination modes of H_3L are various. In the past decade,

(24) Setyawati, I. A.; Liu, S.; Rettig, J.; Orvig, C. *Inorg. Chem.* **2000**, *39*, 496.

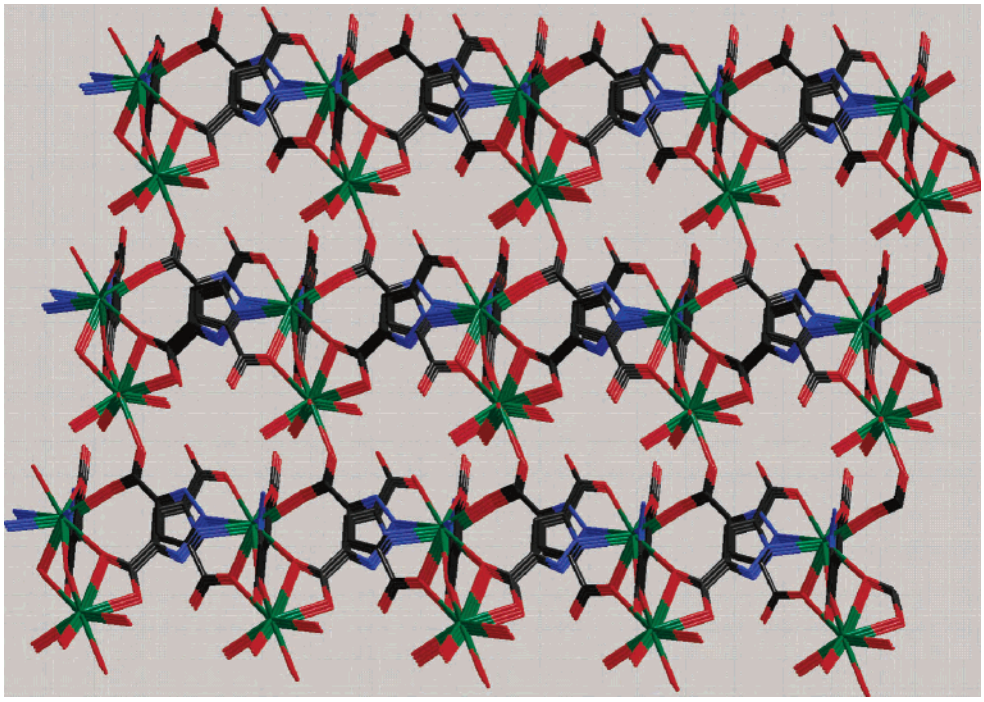

Figure 3. The three-dimensional framework of **1** along the *a* axis. Pr, green; O, red; N, blue; C, gray.

Chart 1. Bridging Modes of the H_3L Ligand. First Observed Coordination Modes in Lanthanide Complexes (**g**−**l**)

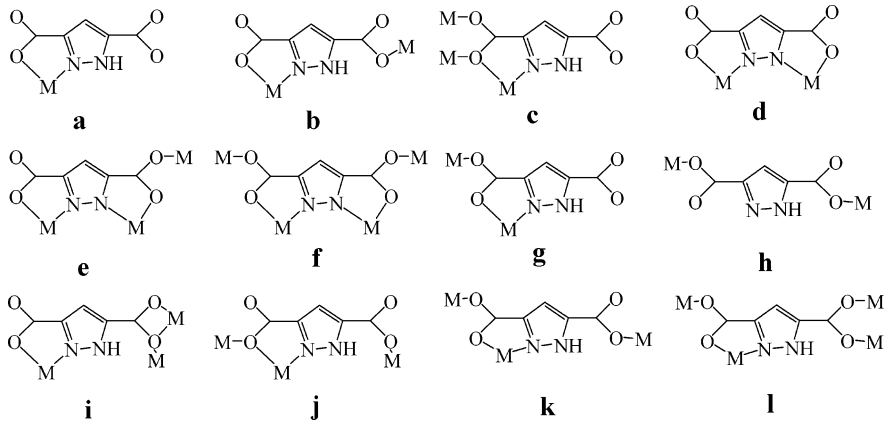

the research on this topic is mainly documented[25] with the transition metals, and to our knowledge, the coordination mode of H_3L with lanthanide complexes has not been reported yet. In this Article, they exhibit more coordination modes (Chart 1). For the Pr complex, there are three different coordination modes (i, j, l) of HL. Such tridentate and tetradentate coordination modes are observed for the first time and play an important role in the assembly of the 3D network.

Crystal Structures of 4−6. The three complexes are also isostructural, and complex **5** is taken as an example to describe the crystal structure. In complex **5**, all of the Gd atoms are eight coordinated and have the same coordination environment (Figure 4). The Gd atom lies in the coordination geometry of a distorted square antiprism with one nitrogen atom and seven oxygen atoms. The nitrogen atom and four oxygen atoms are from HL anions, and the other three oxygen atoms are from water molecules. Notably, only one HL anion coordinated to the Gd atom with both N and O

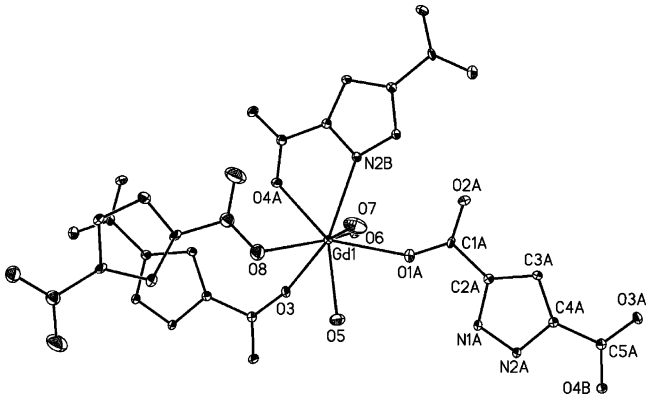

Figure 4. The coordination environment of the Gd atom in **5**. Hydrogen atoms have been omitted for clarity.

(25) (a) King, P.; Clérac, R.; Anson, C. E.; Powell, A. K. *Dalton Trans.* **2004**, 852. (b) Pan, L.; Ching, N.; Huang, X. Y.; Li, J. *Chem.—Eur. J.* **2001**, *7*, 4431. (c) King, P.; Clérac, R.; Anson, C. E.; Coulon, C.; Powell, A. K. *Inorg. Chem.* **2003**, *42*, 3492.

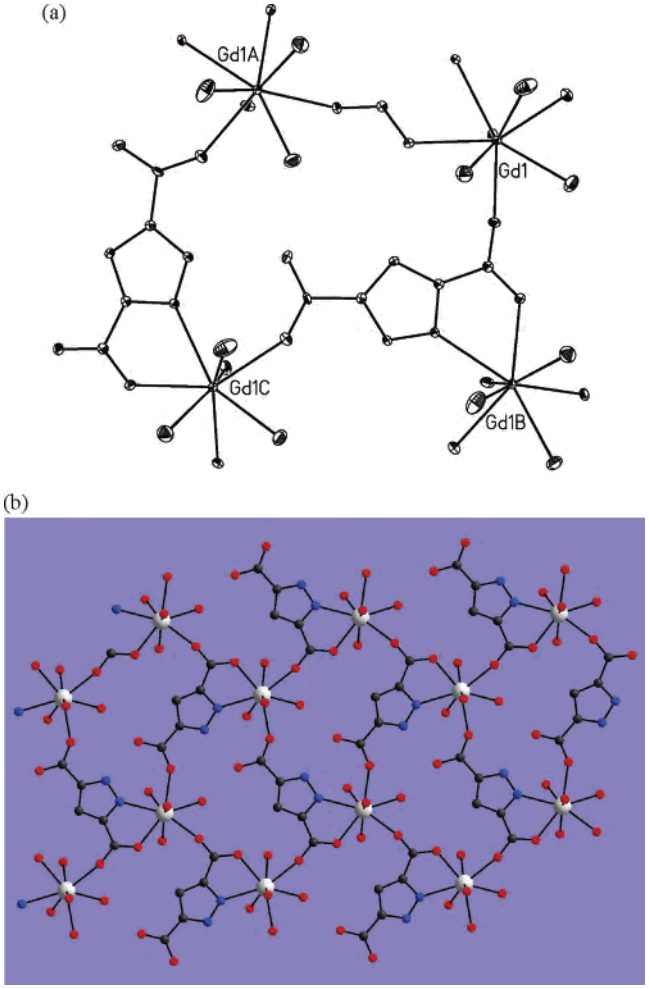

Figure 5. (a) The irregular grid of Gd_4 in the *bc* plane. (b) The 2D grid network architecture of **5** assembled by Gd_4 units in the *bc* plane. Gd, gray; O, red; N, blue; C, black.

atoms at the same time compare to **1**−**3**, and the other three HL anions coordinated to the Gd atom with O atoms. Four adjacent Gd atoms (Gd1, Gd1A, Gd1B, and Gd1C), which are strictly coplanar, form an irregular grid in the *bc* plane, as shown in Figure 5a. The Gd_4 unit repeats in the *bc* plane to form a 2D grid motif (Figure 5b), which is connected to another parallel 2D grid via carboxylate groups of HL anions, resulting in a special 2D double-decker motif (Figure 6). Viewed in the *bc* plane, the bridging HL anions are arrayed regularly between two layers with two different arrangement modes. The plane of one HL anion runs parallel to the others along the *b* axis, and it intersects with the adjacent two planes of the HL anions with the dihedral angle of 44.1° along the *c* axis. The distance between two layers is 6.387(4) Å. In complex **5**, the HL anions have three different coordination modes (k, g, h), which have not been reported.

Crystal Structures of 7−**9.** Among the three isostructural complexes, complex **8** is taken as an example to describe the crystal structure. All of the Ho atoms are eight coordinated with the same coordination environment (Figure 7), which lies in the coordination geometry of a distorted square antiprism with two nitrogen atoms and six oxygen atoms. Notably, four H_3L molecules in **8** are deprotonated to two different types as H_2L^- and HL^{2-}, with the 1:1 ratio, which have not been observed in **1**−**6**. Therefore, each of the HL anions provides a pairs of oxygen and nitrogen atoms, and each of the H_2L ions only provides an oxygen atom. The other two oxygen atoms are from water molecules. Compared with the structures of **4**−**6**, there are two HL anions coordinated with both N and O at the same time. Four adjacent Ho atoms (Ho1, Ho1A, Ho1B, and Ho1c), which are almost coplanar with a mean deviation from the plane of 0.1340 Å, form an irregular square (Figure 8a). The Ho_4 unit as a building block is further assembled into a 2D motif (Figure 8b). In **8**, HL and H_2L anions have two types of bridging modes, b and g (Chart 1). The bridging mode of g has never been observed previously.

Comparison of the Crystal Structures. A comparison of the three different structures is shown in Table 2. In complexes **1**−**9**, lanthanide atoms have two different coordination geometries of distorted tricapped trigonal prisms (the coordination number is nine) and distorted square antiprisms (the coordination number is eight). Although **1**−**9** have the same monoclinic crystal system, they show three different types of crystal structures, which can be classified according to the metal atoms. For **1**−**3**, which form 3D microporous frameworks, the lanthanide atoms (Pr (**1**), Nd (**2**), and Sm (**3**)) belong to the light rare earths. The lanthanide atoms (Eu (**4**), Gd (**5**), and Tb (**6**)) of **4**−**6**, which exhibit special 2D double-decker motifs, belong to the medium rare earths, and for **7**−**9**, which display normal 2D grids, the lanthanide atoms (Dy (**7**), Ho (**8**), and Er (**9**)) belong to the heavy rare earths. With the increasing atomic number of lanthanides, the crystal structures of nine complexes changed from 3D to 2D, and they exhibit three different side views of the 2D grids (**1**−**3**), ladder structures (**4**−**6**), and 1D chains (**7**−**9**),

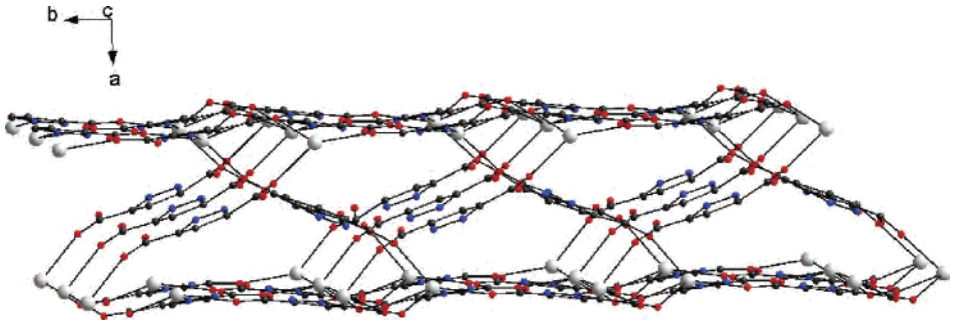

Figure 6. The 2D double-decker motif consisting of two monolayers bridged by HL. The coordinated water molecules are omitted for clarity. Gd, gray; O, red; N, blue; C, black.

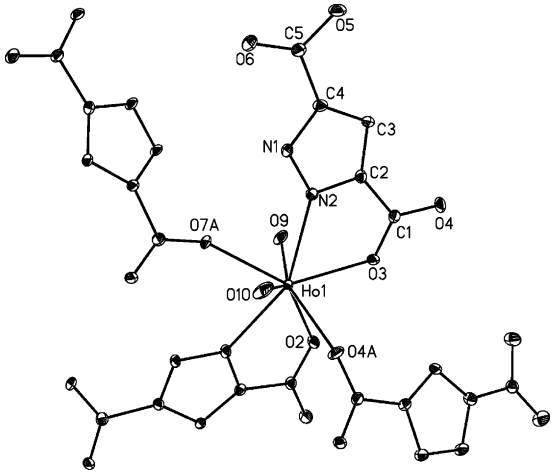

Figure 7. The coordination environment of the Ho atom in **8**. Hydrogen atoms have been omitted for clarity.

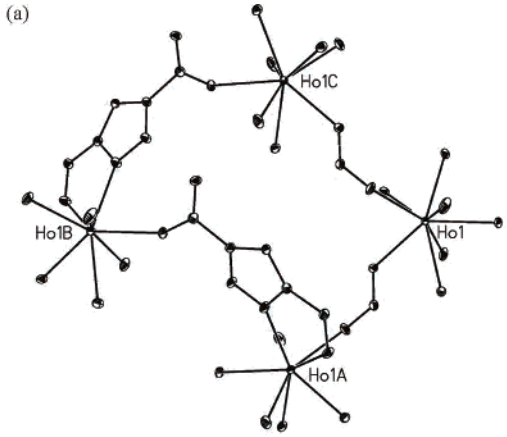

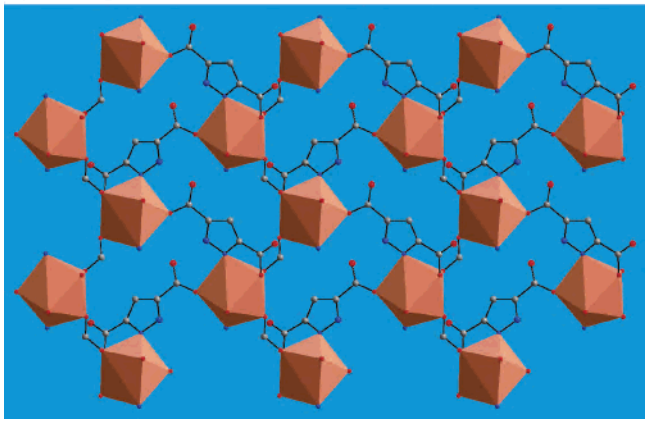

Figure 8. (a) The irregular grid of Ho_4. (b) The 2D motif was assembled by Ho_4 units. Ho, orange; O, red; N, blue; C, gray.

as shown in Figure 9. Combining the above points, it is the lanthanide contraction effect[26] that results in forming the different crystal structures. Moreover, we have compared the average Ln−N and Ln−O bond lengths among the isostructural complexes (Table 2). The average lengths between the lanthanide and N atoms are decreasing continuously from 2.625 (**1**) to 2.449 Å (**9**), and the average lengths between

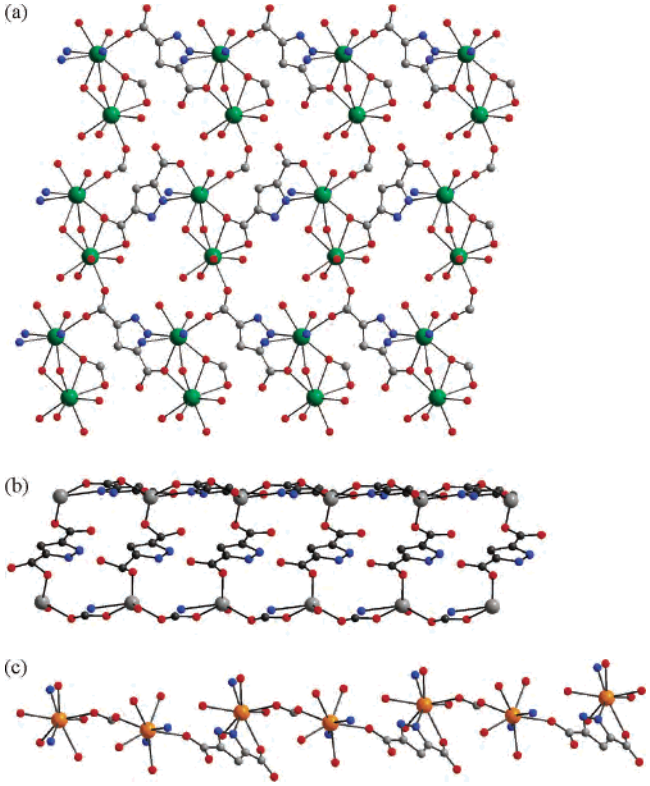

Figure 9. Side view along the *b* axis of three different structures. (a) 2D grid for **1**. Pr, green; O, red; N, blue; C, gray. (b) Ladder motif for **5**. Gd, gray; O, red; N, blue; C, black. (c) 1D chain for **8**. Ho, orange; O, red; N, blue; C, gray.

the lanthanide and O atoms are also decreasing continuously from 2.520 (**1**) to 2.345 Å (**9**).

Luminescent Properties. The luminescent properties of **3**, **4**, **6**, and **7** were investigated in the solid state. The emission spectra of the four complexes (Figure 10) at the excited wavelength of 315 nm exhibit the characteristic emission of Sm^{3+}, Eu^{3+}, Tb^{3+}, and Dy^{3+}, respectively. For **3**, the emission intensity is the weakest, but three characteristic bands can still be observed. They are attributed to $^4G_{5/2} \rightarrow {}^6H_J$ ($J = 5/2, 7/2, 9/2$), $^4G_{5/2} \rightarrow {}^6H_{5/2}$ (568 nm), $^4G_{5/2} \rightarrow {}^6H_{7/2}$ (597 nm), and $^4G_{5/2} \rightarrow {}^6H_{9/2}$ (645 nm) transitions. For **4**, six characteristic peaks are shown in Figure 10b. The three stronger peaks are attributed to $^5D_0 \rightarrow {}^7F_1$ (596 nm), $^5D_0 \rightarrow {}^7F_2$ (616 nm), and $^5D_0 \rightarrow {}^7F_4$ (703 nm), and the three weaker peaks belong to the transitions of $^5D_1 \rightarrow {}^7F_1$ (538 nm), $^5D_1 \rightarrow {}^7F_2$ (560 nm), and $^5D_0 \rightarrow {}^7F_3$ (656 nm). The intensity of the $^5D_0 \rightarrow {}^7F_2$ transition (electric dipole) is stronger than that of the $^5D_0 \rightarrow {}^7F_1$ transition (magnetic dipole), and it indicates that the coordination environment of the Eu^{3+} ion is asymmetric,[27] which is confirmed by crystallographic analyses. For **6**, the emission intensity is stronger than that of the other three in the same conditions. There are four characteristic peaks shown in Figure 10c. They are assigned to the $^5D_4 \rightarrow {}^7F_J$ ($J = 3, 4, 5, 6$), $^5D_4 \rightarrow {}^7F_6$ (491 nm), $^5D_4 \rightarrow {}^7F_5$ (546 nm), $^5D_4 \rightarrow {}^7F_4$ (584 nm), and $^5D_4 \rightarrow {}^7F_3$ (623 nm) transitions. For **7**, two characteristic bands can be seen in the emission spectra, which are

(26) Moeller, T. *The Chemistry of the Lanthanides*; Pergamon Press: Oxford, U.K., 1973.

(27) Kirby, A. F.; Foster, D.; Richardson, F. S. *Chem. Phys. Lett.* **1983**, *95*, 507.

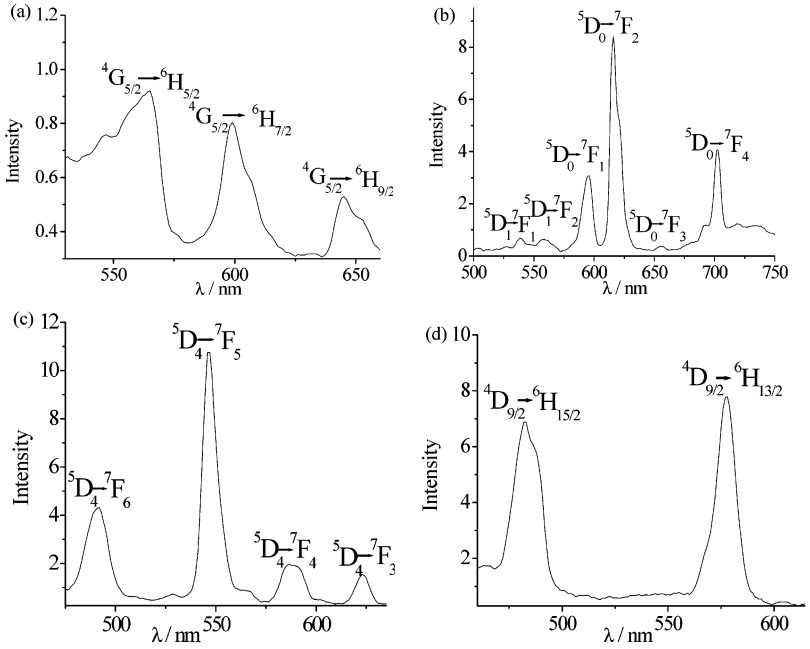

Figure 10. Emission spectra of complexes **3** (a), **4** (b), **6** (c), and **7** (d).

Table 2. Comparison of Complexes **1**−**9**

	1	**2**	**3**	**4**	**5**	**6**	**7**	**8**	**9**
crystal structure		3D			2DD			2DM	
coordination number of M		9			8			8	
kind of M		light rare earth			medium rare earth			heavy rare earth	
bridging mode of L		tetradentate and tridentate			tridentate and bidentate			bidentate	
L_{Ln-N}/Å	2.625	2.610	2.584	2.518	2.513	2.497	2.469	2.467	2.449
L_{Ln-O}/Å	2.520	2.507	2.482	2.386	2.388	2.372	2.361	2.356	2.345
	(Pr)	(Nd)	(Sm)	(Eu)	(Gd)	(Tb)	(Dy)	(Ho)	(Er)

attributed to transitions of 481 nm ($^4D_{9/2} \rightarrow {}^6H_{15/2}$) and 577 nm ($^4D_{9/2} \rightarrow {}^6H_{13/2}$) (Figure 10d). The transition of $^4D_{9/2} \rightarrow {}^6H_{15/2}$ was split into double peaks, which can be observed clearly. It may be the result of the Stark sublevel splitting from the $^6H_{15/2}$ energy level by the ligand field. Compared with the emission spectra of the four complexes (**3**, **4**, **6**, and **7**), the transition intensity changes in the order of Tb^{3+} > Eu^{3+} > Dy^{3+} > Sm^{3+}. It means that the energy transfer from the organic ligands to Eu^{3+} and Tb^{3+} is more effective than that to Sm^{3+} and Dy^{3+}. Furthermore, the intensity of the four complexes based on the H_3L ligand is completely weak, possibly due to the coordinated water molecules, which reduces the luminescent intensity of the rare earth ions,[28] and the energy transfer from the H_3L ligand to lanthanide(III) ions is inefficient in the theory of energy transfer.[29]

Magnetic Properties. The magnetic susceptibility measurement of **5** was performed in the 5−300 K range at a 1 KOe field (Figure 11). At room temperature, the μ_{eff} (the effective magnetic moment) value of 11.19 μ_B is close to the theoretical value of 11.18 μ_B, which is expected for two magnetically quasi-isolated Gd^{3+} ions with $S = 7/2$ ($g = 2.00$). When the temperature decreases, the μ_{eff} value decreases gradually and reduces to 10.18 μ_B at 5 K. The curve is in agreement with an antiferromagnetic behavior of gadolinium complexes. The system is treated with a binuclear approach (based on the spin Hamiltonian $H = -JS_1S_2$), and the least-squares fitting of the experiment data leads to $g = 2.0$, $J = -0.1$ cm^{-1} with the agreement factor $R = 8.9 \times 10^{-3}$. The result indicates that complex **5** exhibits a very weak antiferromagnetic interaction between Gd^{3+} ions. The reason

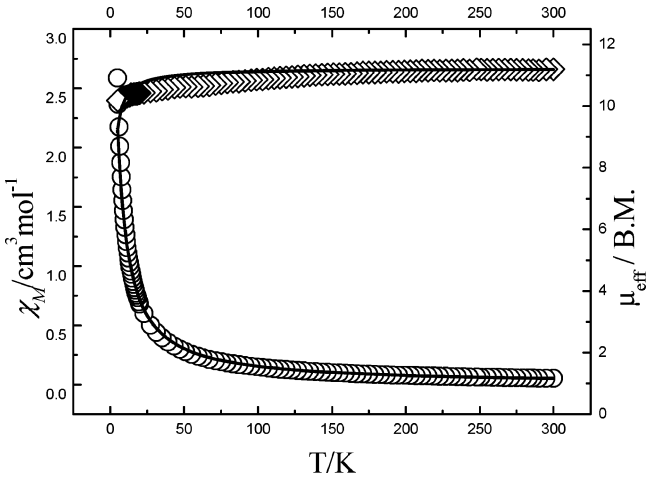

Figure 11. Plots of X_M and μ_{eff} versus T for complex **5**. The square represents the experiment data of μ_{eff}; the circle represents the experiment data of X_M.

(28) Du, C. X.; Wang, Z. Q.; Xin, Q.; Wu, Y. J.; Li, W. L. *Acta Chim. Sin.* **2004**, *62*, 2265.
(29) (a) Dexter, D. L. *J. Chem. Phys.* **1953**, *21*, 836. (b) Brown, T. D.; Shepherd, T. M. *J. Chem. Soc., Dalton Trans.* **1973**, 336.

for the small J value results from the fact that the 4f electrons are influenced very little by the surrounding environment.[30] Theoretically, Gd^{3+} with a $4f^7$ electronic configuration is very stable in energy, and unpaired electrons around Gd^{3+} are very difficult to transfer to the 5d or 6s orbitals of the other Gd^{3+}. On the other hand, the nonzero, overlapped integration between two Gd^{3+} ions would result in an antiferromagnetic interaction within **5**.

Conclusion

Reaction of lanthanide(III) nitrates with the H_3L ligand under hydrothermal conditions results in the formation of nine coordination polymers which can be classified into three types, light rare earth complexes (**1**−**3**), medium rare earth complexes (**4**−**6**), and heavy rare earth complexes (**7**−**9**). Three different types of crystal structures can be isolated based on three groups of rare earth elements for the nine complexes, that is, a 3D microporous framework (3D), a 2D double-decker network (2DD), and a 2D monolayer grid (2DM). It is clear that they changed in the order of 3D → 2DD → 2DM with the increasing atomic number of the lanthanide. Among each group of isostructural complexes (**1**−**3**, **4**−**6**, and **7**−**9**), the average Ln−N and Ln−O bond lengths decrease with the increasing atomic number of the lanthanides, which shows the lanthanide contraction effect. Six new bridging modes from g to l (Chart 1) of the H_3L ligand are observed, which proves that H_3L can be used as an effective bridging ligand in the assembly of MOFs. On the other hand, the complexes of Sm^{3+} (**3**), Eu^{3+} (**4**), Tb^{3+} (**6**), and Dy^{3+} (**7**) exhibit characteristic lanthanide-centered luminescence, and the transition intensity changes in the order of $Tb^{3+} > Eu^{3+} > Dy^{3+} > Sm^{3+}$, which shows the energy transfer from the H_3L ligand to Eu^{3+} and Tb^{3+} is more effective than that to Sm^{3+} and Dy^{3+}. Furthermore, complex **5** exhibits a weak antiferromagnetic interaction between Gd^{3+} ions.

Note Added after ASAP Publication. While this paper was in production, it was found that another paper with similar research results had already been published in *Angew. Chem., Int. Ed.* (**2000**, *39*, 527).

Acknowledgment. This work was supported by the National Natural Science Foundation of China (Grants 20501012, 20631030, and 20425103), the NSF of Tianjin (Grant 06YFJZJC009000), the State Key Project of Fundamental Research of MOST (Grant 2005CCA01200), and MOE (Grant 20060055039) of China.

Supporting Information Available: CIF and bond lengths and angles for complexes presented in this paper. This material is available free of charge via the Internet at http://pubs.acs.org.

IC061620P

(30) Molina, M. H.; Pérez, C. R.; López, T.; Lloret, F.; Julve, M. *Inorg. Chem.* **2003**, *42*, 5456.